LUNG RESPONSE AND INJURY IN SIDE IMPACT CONDITIONS

K. F. Yuen[1], D. S. Cronin[1], Y. C. Deng[2]
University of Waterloo[1], General Motors Corp.[2]

ABSTRACT

Lung injury was investigated using a 50th percentile male finite element human body model, including a previously developed detailed thorax, subject to lateral pendulum impacts. Improved geometric representations of the lung and heart were implemented in the model and the finite element mesh quality and contact interaction with adjacent anatomical structures was improved. The model was validated against experimental impact tests using force and compression response. Pulmonary contusion was predicted based on four injury metrics, and found to be consistent with predicted AIS levels using the Viscous Criterion.

Keywords: SIDE IMPACT, THORAX, PULMONARY CONTUSION, FINITE ELEMENT METHOD, INJURY CRITERIA

THORACIC TRAUMA, particularly in side impact conditions is an important issue to understand in terms of injury prediction to improve occupant protection. In 2006, there were almost 6 million police reported crashes resulting in 36902 vehicle occupant fatalities and nearly 2.5 million injuries in the United States (NCSA, 2006). Among those fatalities and injuries, side collision as the initial point of impact accounted for approximately 25.3% and 25.7% respectively. In 2001, side impact collision resulting in thoracic injury accounted for 38% of the fatalities and 59% of non-fatal injuries (NHTSA, 2004). Pulmonary contusion was identified as the most common injury following blunt chest impact (Gayzik, 2007).

Thoracic response to blunt impact has been widely studied in the literature (Kroell 1974; Lau 1985,1986; Viano 1998, 1989a, 1989b; Cavanuagh 1990a, 1990b, 1993, 1994; Pintar 1997; Kuppa 1998), along with many advanced model developments (Deng, 1999, Chung, 1999, Chang 2001, Lee 2001, Yang, 2003, Ruan 2003, 2005). However, occupant response is often characterized based on global measures including force and deformation; whereas, the ultimate goal of detailed human body models is to predict thoracic response and injury at the organ level. Similar approaches have been proposed for brain injury (Stitzel et al., 2002; Takhounts et al., 2003), abdominal injury (Sparks et al., 2007) and lung injury (Stitzel, 2005; Gayzik, 2007). Experimental developments at the organ or body region level can be used to verify and validate finite element human body models for predicting localized injury. Important studies in this area related to blunt thoracic trauma modeling include Happee (1998), Furusu et al. (2001), Thollon et al. (2002), Ruan et al. (2003), Yang et al. (2003).

The objective of this study was to enhance an existing detailed finite element human body model (Deng 1999, Chung 1999, Chang 2001, Forbes 2006) to predict lung response and correlate it to injury. Impact loading was applied using pendulum impact tests and evaluated using common injury criterion such as chest compression, impact force, and the Viscous Criterion (VC).

THORACIC TRAUMA

The prediction of thoracic trauma requires measurable parameters to be correlated to different injury levels. Injuries to the body are often classified or graded according to the Abbreviated Injury Scale (AIS), which numerically classifies the level of injury sustained by a body region or organ (States, 1969; AIS 2005). Table 1 shows typical injuries to the lung as categorized by the AIS. Due to the challenges in measuring tissue response and damage at a localized level, injuries are commonly predicted through global measurements such as chest compression, impact force, and chest acceleration. This has been the focus of the currently accepted injury criteria (Kuppa and Eppinger, 1998). Common criteria include the Thoracic Trauma Index (TTI) (Eppinger et al. 1984), the Blunt Criterion (BC) (Sturdivan et al., 2004) and the Viscous Criterion (VC) (Viano, 1985). For the

purposes of this study we have focused on the Viscous Criterion due to the availability of PMHS data, measured response, and correlation to AIS. Future work will include evaluation of TTI and BC.

Table 1. Lung AIS Level Summary & Description (AIS, 2005)

Grade	Injury Description		AIS
I	Contusion	Unilateral, <1 lobe	3
II	Contusion	Unilateral, single lobe	3
	Laceration		
	Laceration	Simple pneumothorax	3
III	Contusion	Unilateral, >1 lobe	3
	Laceration	Persistent (>72hrs), airleak from distal airway	3-4
	Haematoma	Nonexpanding intraparenchymal	3-4
IV	Laceration	Major (segmental or lobar) airway leak	4-5
	Haematoma	Expanding intraparenchymal	4-5
	Vascular	Primary branch intrapulmonary vessel disruption	3-5
V	Vascular	Hilar vessel disruption	4
VI	Vascular	Total, uncontained transaction of pulmonary hilum	4
Note: Advance one grade for bilateral injuries. Haemothorax is graded by thoracic vascular organ injury scaling.			

VISCOUS CRITERION The Viscous Criterion (VC) was formulated by Lau and Viano (1985) to evaluate the risk of soft tissue injury defined by the instantaneous product of velocity of deformation and normalized compression of the thorax. Using this criterion, Viano and Lau (1988) proposed $[VC]_{max}$ values for frontal injury levels based on PMHS experiments (Kroell et al. 1974). Viano et al. (1989a, 1989b) subjected PMHS to off-angle pendulum impacts to develop lateral injury criteria. The VC response was correlated to AIS level probabilities. The results of the experiments are provided in Table 2 (Viano et al., 1989b). These test cases were used as the basis for the current study.

Table 2. Viscous Criterion associated with AIS level (Viano et al., 1989b)

Injury Level	25% Probability	50% probability
Lateral $[VC]_{max}$ (m/s)		
AIS $\geq$ 3	Data not available	1.00
AIS $\geq$ 4	1.47	1.65

LOCAL INJURY PREDICTION Lung injury can generally be classified as laceration or contusion. Contusion occurs when lung tissues are damaged due to blunt impact resulting edema or/and hemorrhage. Fung et al. (1988) and Yen et al. (1988) investigated the injury mechanism of pulmonary contusion and suggested that the injury is caused by the compressive stress waves resulting from the impact. Although the injury mechanism at the alveolar level has been investigated by many authors, it is still not fully understood.

Miller et al. (2001) conducted a study to quantify pulmonary injury relative to pulmonary function and outcome. 49 patients (35 bilateral) with pulmonary contusion (PC) from isolated chest trauma were measured using computed tomography (CT) scans and showed contusion levels ranging from 5% to 55% based on volume, the mean contusion volume for the entire group was 18%. From Miller et al.'s regression analysis, patients were classified with severe PC suffering from high risk of pulmonary dysfunction when the lung contusion volume was greater than 20%.

Development of an injury metric that can predict pulmonary contusion is necessary for advanced numerical human body models. Stitzel et al. (2005) and Gayzik et al. (2007) have been investigating a rat model to correlate experimental impact and pulmonary contusion using CT scan data. In parallel, a finite element model was developed to investigate lung tissue mechanical response. Gayzik

et al. (2007) found that predicted contusion levels based on the product of maximum principal strain times strain rate correlated with measured contusion. Principal strain and strain rate were also found to provide reasonable estimates of contusion levels based on the experimental data.

Yen et al (1988) had found evidences of hemorrhagic injury in the lung are localized and are usually most severe next to the spine, heart, ribs or at the edges of lobes. Yen also suggested the importance of the wave feature of the phenomena: high stress concentration, focusing, reflection, and localization. Dynamic pressure was evaluated in this study as a candidate injury metric since it captures stress wave propagation through the lung. Stuhmiller et al (1988) and Josephson et al (1988) have suggested the existence of a threshold lung pressure level above which trauma will occur. Greer (2005), Cronin (2004) quantified different levels of injury in the lungs under blast environment by evaluating dynamic pressure in the lung tissue through their FE model. The pressure thresholds were developed through FE analysis by comparing model response to the injury outcome of the experiments by Bowen (1968) where sheep were subjected to blast loading. A relationship between dynamic pressure and injury was established through Salisbury et al (2006) as shown in table 3.

Table 3. Dynamic Pulmonary Pressure Levels and Associated Injury (Salisbury, 2006)

0-60 kPa	None
60-100 kPa	Trace
100-140 kPa	Slight
140-240 kPa	Moderate
>240 kPa	Severe

METHODS

This study builds on a fourth generation thorax FE model (Deng et al. 1999, Chung 1999, Chang 2001, Forbes et al. 2006). The thorax model was developed to predict thoracic response and to study injury mechanisms in vehicle impact scenarios. The finite element model includes a detailed representation of the thorax and the upper limbs. Digital surface images (Viewpoint Data Labs) of the human body were used to construct the three-dimensional finite element representation of the thorax including heart and lungs. A simplified head, abdomen, pelvis, and lower limbs were also implemented to allow for full body kinematics during an impact scenario. A shoulder model with representative musculature was also developed and found to be critical to accurately predict global thoracic response in side impact scenarios (Forbes, 2006).

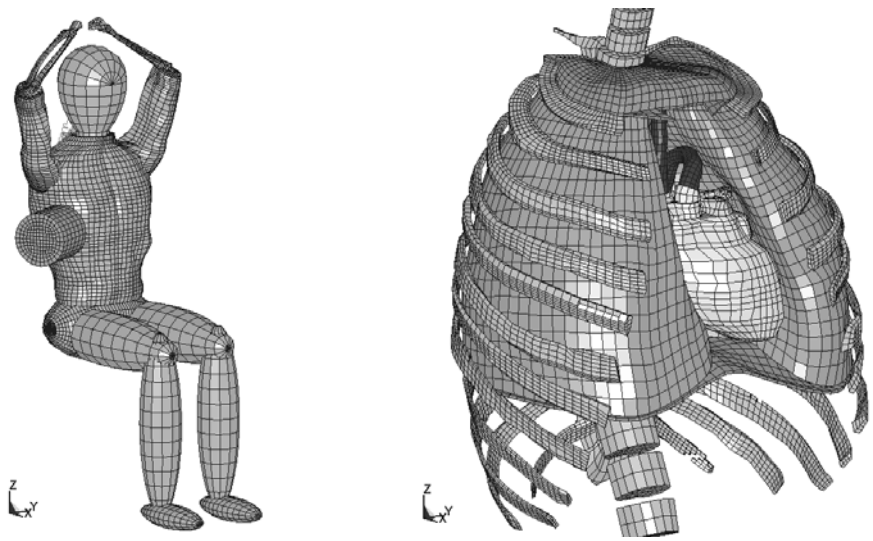

(a) **(b)**

Fig. 1 - FE Full Body Model (a) side pendulum setup (b) exposed view of thorax

Initial studies using the latest version of the model showed that the global responses (force, deflection) were good for pendulum impact scenarios. It was found that the outer muscle tissue and the intercostal tissue had significant influence over the gross response of the thorax, which is consistent with a previous study done by Murakami et al. (2006). Several areas were identified for improvement of the internal organs including overall geometry, finite element mesh quality and density, and interfaces with adjacent organs and structures. The latter aspect was considered important to improve stress wave transmission and response. Improvements to the lung model were based on geometric data from the Visible Human Project (National Library of Medicine, 2004). The improved lung model consists of 11669 elements with more than 84% having a Jacobian value of 0.7, and approximately 90% having an aspect ratio less than 3. Element size, hourglass control, contact interaction, and material parameters were considered when developing the lung model with the primary challenges being low density, low wave speed, and potentially high deformations during impact scenarios. An exposed view of the thorax region is shown in Figure 1.

LUNG CONSTITUTIVE MODEL The lungs were modeled as a continuum using 8-noded brick elements with an average element size of 8mm. The selection of element size is discussed further below. The constitutive model proposed by Fung et al. (1978) and Vawter (1980) was used for this study (Equation 1) where the elastic properties are modeled by a strain energy function (first term in Equation 1). C, C_1, C_2 α, β are material constants, Δ is the typical alveolar diameter when unstressed, and I_1 and I_2 are the strain invariants. PMHS lung tissues were tested using the biaxial tensile test apparatus at the University of Memphis (Yen, 1999) to provide numerical values for C/Δ, α and β. The surface energy coefficients C_1/Δ and C_2 were adopted from Vawter (1980). The parameters used in the material model are listed in Table 4.

Equation 1. Strain Energy Function (Vawter, 1980)

$$W = \frac{C}{2\Delta}\exp(\alpha I_1^2 + \beta I_2) + \frac{12C_1}{\Delta(1+C_2)}[A^{(1+C_2)} - 1]$$

$$A^2 = \frac{4}{3}(I_1 + I_2) - 1$$

$$I_1 = e_{11} + e_{22} + e_{33}$$

$$I_2 = e_{11}e_{22} + e_{22}e_{33} + e_{33}e_{11} - e_{12}^2 - e_{23}^2 - e_{31}^2$$

Table 4. Lung Material Model Summary

C/Δ [kPa]	α	β	C_1/Δ [kPa]	C_2	P [kg/m^3]	K [kPa]
0.592	5.85	-3.21	0.0193	2.71	200	24500

Bowen et al. (1968) measured lung material density to be approximately 200 kg/m^3. Based on the improved geometry in this model, the current right lung mass is 615g and the left is 562.7 g. This is in agreement with Gray (1918) who estimated average the right lung weight to be 625 g and the left lung weight to be 567 g. The speed of a stress wave propagating through an inflated lung ranges from 30 to 40 m/s (Fung 1985, Yen, 1986) with a corresponding bulk modulus of 2.45X10^5 Pa , which is lower than most soft tissues. Past research (Fung, 1985; Yen, 1986; Grimal, 2002) has shown that lung density depends significantly on the transpulmonary pressure and blood or serous fluid within the lung. Initial studies showed that model instability could occur for higher rate impacts when using a typical bulk modulus and treating the bulk response as linear. For this study, a bulk modulus of 24500 kPa was used, and future studies will focus on nonlinear treatment of compressibility, which is important for impact conditions.

LUNG MESH CONVERGENCE A lung mesh convergence study was undertaken to assess mesh dependence and response under representative loading conditions. A 160 mm diameter, 80 mm length cylinder of lung material was deformed with a prescribed velocity 6.5 m/s to provide 50% nominal deformation within 20 ms to simulate typical impact conditions. The model response was investigated for four different element sizes (2.5 mm, 5 mm, 10 mm, and 20 mm). Distribution of element response in terms of % volume was compared for pressure, principal strain, and principal strain rate as shown in Figure 2. For each response metric, a corresponding volume fraction represented the percentage of elements that had a peak response at that level or lower.

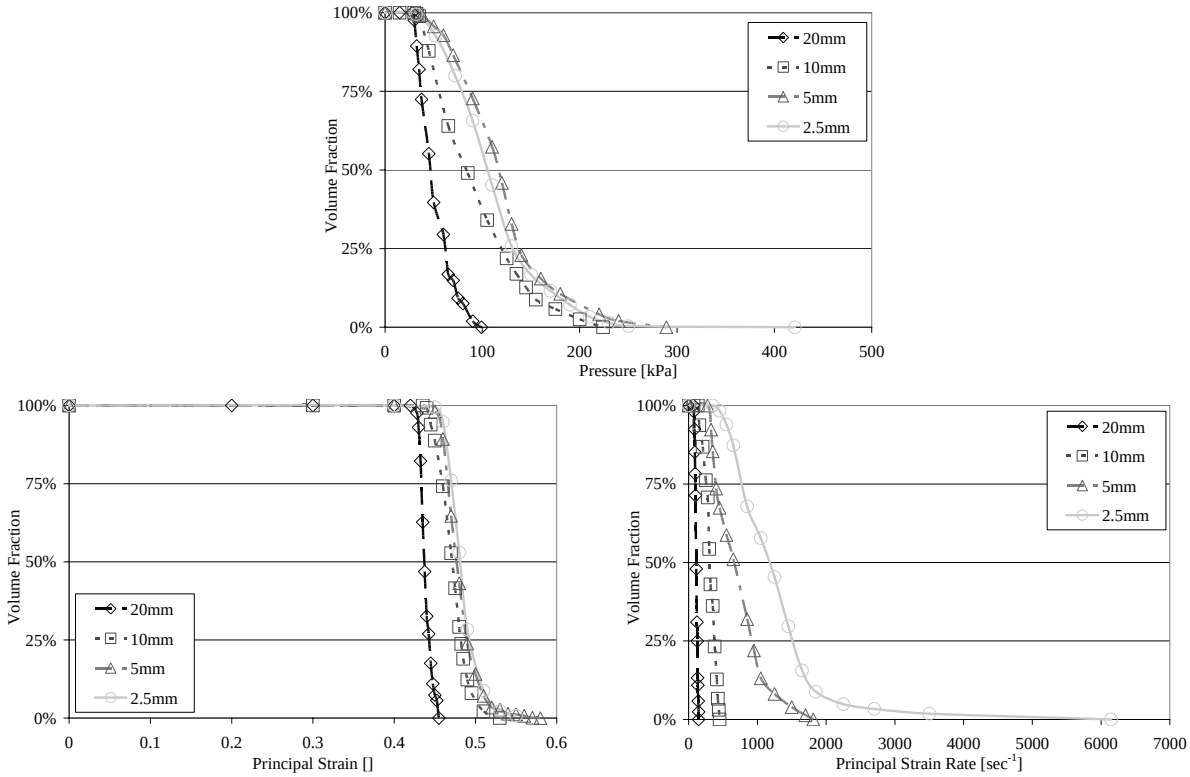

Fig. 2 - Mesh Convergence - Pressure, principal strain, and principal strain rate peak response distribution.

The results showed that the range of peak principal strain response was relatively constant across the volume of the material, with a trend towards convergence with smaller element size. Principal strain rate becomes less linear with a trend towards larger strain rate with smaller element size. In contrast, the dynamic pressure demonstrated a consistent trend between element sizes for elements smaller than 10 mm.

This convergence study concluded that response can be highly dependent on mesh density, with strain and pressure response being least dependent and principal strain rate being most dependent on element size. The corresponding injury predictions would also show these same dependencies, and must be considered when selecting an injury metric. Based on these results, the lungs were meshed with an average element size 8 [mm] with maximum element size no larger than 10 mm. This allowed for consistent prediction of response, and an additional study showed that this was acceptable in terms of computation time.

MODEL VALIDATION During the development of this thoracic model, Forbes (2006) validated it against various types of impact experiments such as frontal thoracic pendulum impact (Kroell, 1975), limited stroke impact test (Chung, 1999), NHTSA Side Sled tests (Pintar, 1997), Wayne State University side sled tests (Cavanaugh, 1990a, 1990b, 1993, 1994), and pelvic and abdominal

pendulum impacts (Viano, 1989b). Forbes (2006) demonstrated the model response was in good agreement with the experimental response corridors for these studies, based on the ISO biofidelity ratings.

For the current study, lateral blunt pendulum impacts on PMHS (Viano, 1989b) were used to provide a comparison to the predicted thoracic response. The experiment used a free flight 23.4kg, 15cm diameter pendulum aligned with the thorax at 30 degrees from lateral axis. The center of pendulum impact on the thorax was aligned with the xiphoid process in the horizontal plane. The impact axis was directed at the center of gravity of the torso and the pendulum impacts occurred at three different velocities, 4.4 m/s, 6.5 m/s, and 9.5m/s.

Table 5. Normalized Cadaver Response (from Viano, 1989b)

Peak Thorax Response	4.4m/s	6.5m/s	9.5m/s
Force [kN]	**2.67 +/-.99**	**3.1 +/-.46**	**6.30 +/-.90**
Deflection [cm]	**8.40 +/-1.3**	**11.20 +/-1.35**	**14.18 +/-1.79**
Compression [%]	**26.1% +/-4.1**	**34.9% +/-4.5**	**43.2% +/-3.9**
VC [m/s]	**0.62 +/-.23**	**1.10 +/-.18**	**2.05 +/-.41**
AIS	**.4 +/-.9**	**2.8 +/-.5**	**4 +/-.6**

Table 6. Thorax Model Response

Peak Thorax Response	4.4m/s	6.5m/s	8.5m/s
Force [kN]	**2.40**	**3.83**	**5.44**
Deflection [cm]	**8.5**	**11.3**	**12.7**
Compression [%]	**25.4%**	**34.3%**	**38.1%**
VC_{max} [m/s]	**0.47**	**1.00**	**1.52**

Table 5 shows a summary of the PMHS response for the three impact velocities. Table 6 shows a summary of the predicted model response under similar impact conditions. Overall, the peak force, deflection, compression, and VC were in good agreement with the PMHS experimental data reported by Viano. The force and deflection responses were within the experimental corridors; however, the short duration (less than 5ms) force response was generally higher than that measured for the PMHS subjects. Model instability occurred for the 9.5 m/s pendulum impact simulation due to severe deformations, so an 8.5 m/s case was investigated to provide response for a high level impact.

CANDIDATE INJURY METRICS Fung et al. (1988) proposed different metrics to quantify injury such as shear stress, octahedral shear stress, maximum principal strain, maximum shear strain, triaxial mean strain, strain rate, and the instantaneous product of the strain and strain rate. Gayzik et al. (2007) evaluated these metrics and concluded that the product of max principal strain times strain rate correlate best to the distribution of pathology from the CT analysis. The maximum principal strain and its strain rate were the second and third best fitting metrics. Under blast environment, injury metric for lung injury is often measured in terms of intrapulmonary pressure (Salisbury, 2006, Greer, 2005, Cronin, 2004). In this study, four measures of lung response were used to predict pulmonary contusion including principal strain, principal strain rate, product of principal strain times its strain rate, and dynamic pressure. All response traces were not filtered. The lung response from each impact case was predicted from the stress and strain tensor of all lung elements for times from 0ms to 60ms after the impact. Metrics were calculated for the lung elements over this time span and used for comparison to expected lung contusion volumes based on the measurements by Miller (2001).

The post-impact contusion volume observed in the lung model was correlated to the four different candidate injury metrics. All traces were output at .025 ms intervals to ensure adequate resolution for capturing peak pressure and strain rates. For each metric, the peak value of each element over the 60ms time span was recorded. For a given metric, elements whose value was either above or below a

threshold were partitioned into two groups: one predicting contused parenchyma, and the other representing normal parenchyma.

The proposed thresholds for all candidate injury metrics were determined based on the 6.5m/s pendulum impact, where the AIS level was approximately 3. Miller et al. (2001) suggested that lung contusion over 20% can be classified as severe pulmonary contusion. As an initial assessment, the candidate metric threshold values were determined corresponding to 20% contusion volume for the 6.5 m/s impact scenario. These selected thresholds were then used to evaluate contusion volume at other pendulum impact velocities of 4.5 and 8.5 m/s. This approach to determine the injury thresholds was selected to provide an understanding of the differences between the injury metrics and response at different impact velocity levels.

RESULTS

The current numerical model builds on the hypothesis that lung tissue can be classified as contused when it exceeds a given threshold for the injury metric, and that the total volume of contused lung tissue dictates the severity of the lung injury. The validated full body numerical model was used to explore localized lung model responses when subjected to different pendulum lateral impact velocities. In this study, three impact velocities 4.5 (low), 6.5 (med), and 8.5 (high) m/s were simulated for comparison to previous PMHS side impact pendulum tests studies (Viano 1989b).

The principal strain, strain rate, and pressure for each element were recorded for the three different impact velocities. Table 7 summarizes total contused lung volume prediction (both lungs) for each metric, where the 6.5m/s impact case was used as the baseline for 20% contusion. The percentage of contused volume that exceeded the threshold for each lung is shown in Table 8.

Table 7. Total Lung Contusion Volume Summary, % based on volume of both lungs

Peak Thorax Response	Total Contusion Volume %		
	4.4m/s	6.5m/s	8.5m/s
Strain	1.3	20.0	33.8
Strain Rate	0.1	20.0	37.6
Strain*Strain Rate	2.0	20.1	37.6
Pressure	1.4	20.0	39.5

Table 8. Individual Lung Contusion Volume Summary, % based on individual lung volume

Peak Thorax Response	Threshold	Individual Lung Contusion Volume %					
		4.4m/s		6.5m/s		8.5m/s	
		Non-struck side	Struck Side	Non-struck side	Struck Side	Non-struck side	Struck Side
Strain	0.525	0.0	2.5	1.1	38.2	5.8	59.3
Strain Rate [s^{-1}]	311	0.0	0.1	2.1	36.6	6.2	66.4
Strain*Strain Rate [s^{-1}]	95	0.3	3.6	1.1	37.5	6.0	66.4
Pressure [kPa]	157	0.0	2.7	0.3	38.5	1.3	74.5

Figure 3 summarizes the predicted peak value distribution for each injury metric for all three impact scenarios. Figure 3 (a) shows the distribution in the left lung, far side from the impact, where as (b) shows the distribution in the right lung, struck side of the impact. Results show that all metrics predict only modest damage levels for the non-struck side. Most of the contused lung volume was situated at the struck side of the thorax, which was the right lung for all three impact scenarios.

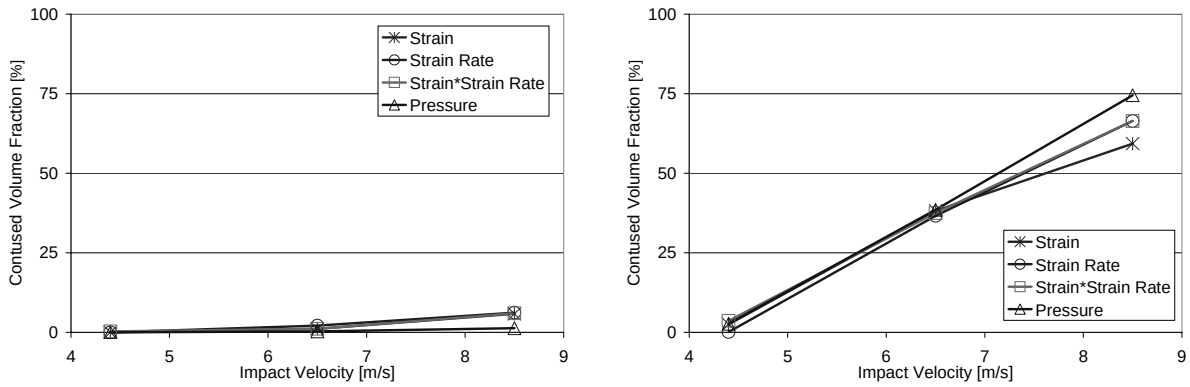

Fig. 3 – Contused Volume Response under Three Velocities
(a) Far Side–Left Lung (b) Struck Side–Right Lung

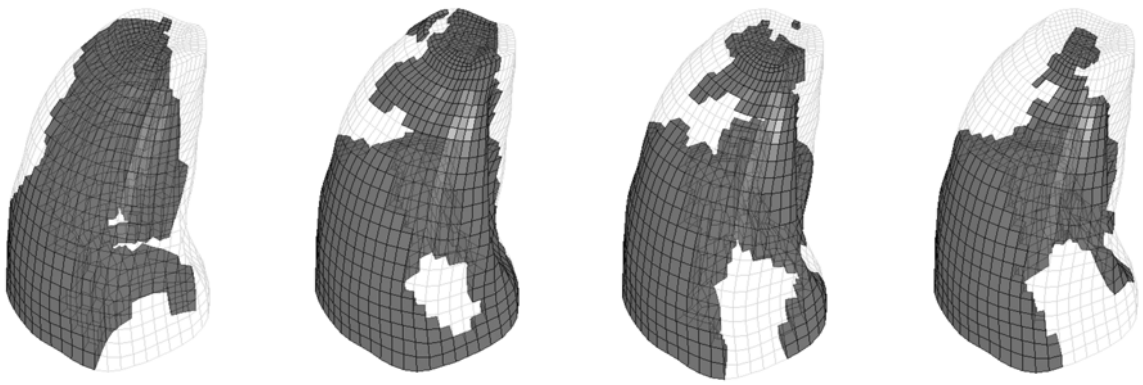

(a) (b) (c) (d)

Fig. 4- Predicted Lung Contusion Plots (Right lung, 6.5 m/s impact) - (a) Principal Strain (b) Principal Strain Rate (c) Product of Principal Strain and its Strain Rate (d) Pressure

Figure 4 shows contour plots of the lungs for each metric under the 6.5m/s impact case. Given that each metric corresponded to 20% contusion based on volume, the injury patterns showed some similarities. The most severe injury was predicted at the impact location, with only modest levels of injury in the left (non-struck) lung. Figure 4(a) displays the predicted strain response where the primary injured section is aligned with the pendulum impact axis. The surface at the opposite side (along the spine) of the impact location was also predicted being contused. Figure 4 (b) displays the predicted strain rate response where the significant injury locations were near the struck and opposite sides of the struck lung, along the impact axis. The surfaces contacting the heart were predicted as the secondary injury locations. Figure 4 (c) displays the product of strain and strain rate where primary and secondary injury locations were similar to strain rate only response. Figure 4 (d) displays the predicted pressure response where the primary injury locations were in line with the impact axis near the struck side and opposite sides of the struck lung and more concentrated at the inferior section of the lung . The contused volume was more dominant in the struck side of the lung. Despite the geometry and simplified attachment points in the model, (i.e. trachea, bronchi, pulmonary veins not modeled), no significant injury was associated with these locations and this is consistent with observed injuries (Miller 2008). Yen et al (1988) suggested injury in the lung is typically localized; occur next to the spine, heart, ribs, or at the edges of lobes. The model predictions are in agreement with these findings.

Figure 5 shows the distribution, in terms of cumulative percentage volume, for the four injury metric candidates. For each response metric, a corresponding volume fraction represented the accumulative percentage of the struck-side lung model elements that had a peak response at that level or higher.

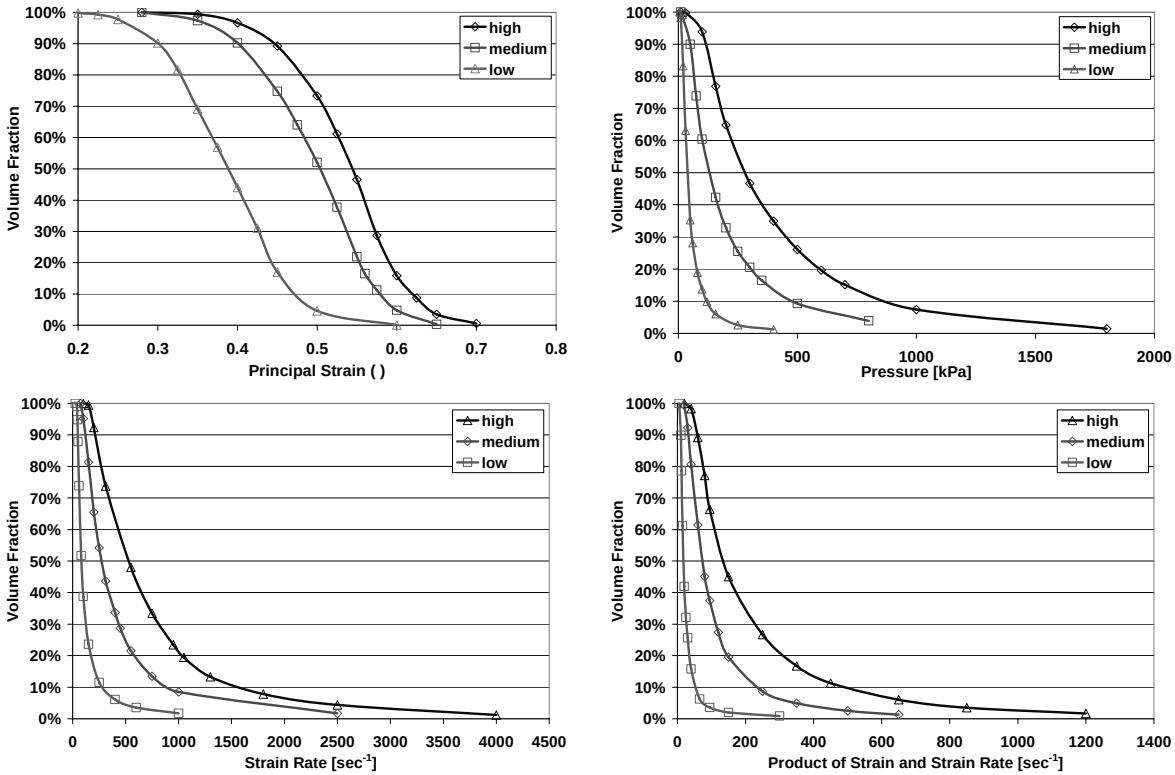

Fig. 5 - Peak Response Distribution – a) Principal Strain b) Pressure c) Principal Strain Rate d) Instantaneous Product of Principal Strain and its Strain Rate

DISCUSSION

Side pendulum impacts were simulated for three different velocity conditions, and the response of the lung was evaluated based on mechanical response and four injury metrics. Based on the current study, the proposed injury thresholds for principal strain, principal strain rate, the product of principal strain times strain rate, and pressure to be .525, 311 s^{-1}, 95 s^{-1}, 157 kPa, respectively. The proposed thresholds for principal strain, principal strain rate, and the product of principal strain times strain rate by Gayzik (2007) are .154, 304 s^{-1}, and 28.5 s^{-1}, respectively. The discrepancy between the thresholds is tied to the dependence of strain and strain rate response to mesh size, material model parameters, and loading conditions. Gayzik (2007) also emphasized that his model's parameter set may not be valid to conditions that are different than its experiments and the proposed thresholds are dependent on the material model. Previous work on the pressure level threshold for blast injury (Cronin 2004) provided lung contusion thresholds ranging from 60-100 kPa (trace) to 240 kPa or above (severe), in agreement with the findings for this model.

This model predicted significant localized deformation in the lungs, particularly at the struck location. The range of pendulum impact velocities and corresponding AIS levels provided a broad range of conditions to evaluate lung injury. The results show that the predicted lung peak response values are consistent when considering pressure, strain rate and the product of strain and strain rate. Further, the selection of an injury metric based on the actual lung contusion injury mechanism still requires investigation. The contusion volume can be estimated from these results across different impact levels based on the injury thresholds selection.

All four injury metrics showed relatively similar predicted lung contusion volumes across the three impact scenarios, except strain which predicted lower levels of contusion for the high velocity impact case. The primary location of lung contusion was at the impact location on the struck lung, as expected. The torso model predicted a VC_{Max} of 1.00 at medium velocity impact, which coincidentally correlates to 50% probability at AIS level 3 according to Viano's study (1989b). From Viano's study, a VC_{Max} of 1.65 correlates to 50% probability of an AIS level 4. The VC_{Max} was 1.52 for the 8.5 m/s

impact case, with a predicted lung contusion volume almost double (~34% to 40%) that of the medium impact scenario (~20% total contusion volume). This suggests that there is significant lung contusion volume increase when going from AIS level 3 to 4, in agreement with the study by Miller et al. (2001) where the contusion volume of admitted patients ranged from 5% to 55%. Although total contusion volume was 20% considering both lungs, this study shows that lung contusion occurs primarily to the lung on the struck side. The right lung contusion volumes ranged from 36.6% to 38.5% and would likely disrupt pulmonary function in more than one lobe of the struck lung.

Severe impacts are typically correlated with multiple rib fractures, and this was also predicted by the model. The model predicted 3 rib fractures at low velocity impact, 8 rib fractures at medium velocity, and 15 rib fractures at high velocity, comparable to the PMHS study (Viano 1989b). This study showed that more severe impacts, which lead to rib fracture, also generate significantly higher levels of contusion injury. The fractured rib corresponds to sudden loss of ribcage stiffness which leads to localized deflection at the fractured site in addition to the deformation from impact event. When strain rate or pressure response are monitored, sudden loading due to fractured rib can be observed as a stress wave initiates at the fractured rib location and propagates through the lung. Peak responses of the stress wave do exceed the threshold defined by this study, showing that the fractures can increase the severity of lung injury.

A mesh convergence study showed that strain and strain rate behavior were more dependent on mesh density; and the corresponding volume thresholds were also affected by mesh density. Pressure was found to be a more consistent measurement across the different mesh densities. Due to the transient nature of the pressure response, appropriate material modeling was required to accurately predict the wave propagation effect. In general, strain, strain times strain rate, and peak pressure provided similar responses while the strain-only measure did not adequately capture the rate effects.

LIMITATIONS OF THIS STUDY This study highlights the importance of representative tissue geometry and constitutive models, as well as consistent mesh density across the model to predict internal organ response. The presented numerical results are limited by the current lung constitutive data. In addition, further improvements could be realized through validation using experimental data following the approach as Stitzel et al. (2006) and Gayzik et al. study (2007) but over a greater range of loading conditions. A direct correlation cannot be drawn with Stitzel and Gayzik's study as current proposed injury thresholds are dependent on a specific material model and loading condition. Despite the differences, the strain rate threshold proposed by Gayzik et al. study is 304 sec^{-1} whereas the current study proposed 311 sec^{-1}. There is evidence to suggest that lung response should be rate dependent, similar conclusion was drawn by Gayzik et al. study. There is still more development required to establish the dominant mode of lung tissue damage under blunt impact scenarios. In addition, further studies should be undertaken to build on the work by Miller in identifying injury patterns to correlate the amount of contusion to each lobe in the lungs and any functional disruptions.

CONCLUSIONS

Human torso response and lung injury from pendulum side impacts has been studied using finite element simulations of PMHS cadaver experiments. The predicted response of the full body model was in good agreement with the experimental results in terms of peak response, force-time and force-deflection characteristics. The goal of this study was to assess lung injury based on predicted response of the lung using a detailed finite element thorax model. Four injury metrics were investigated to predict lung contusion over a range of pendulum impact velocities. A separate mesh convergence study was conducted among the four metrics, and showed that strain response was highly mesh size dependent while dynamic pressure was the least mesh dependent. Strain rate, the product of strain and strain rate, and pressure provided approximately similar levels of lung contusion volume for all three impact scenarios, with strain response under predicting contused lung volume. Lung contusion was also predicted to increase significantly for impact scenarios going from AIS level 3 to AIS level 4. All four metrics identify the likelihood of tissue contusion at the struck location and opposite side of the struck lung, along the impact axis. Under lateral impact, lung contusion was primarily predicted in the lung at the struck side of the thorax with only a modest amount of contusion in the opposite lung, even at high impact velocities. Additional loading and injury was observed correlating to rib fracture at the impact location. Predicted secondary contusion locations were

different for all four metrics, but typically at interfaces with other tissues in the thorax. Continued research will focus on developing an improved constitutive material model for the lungs, and comparison to injury patterns in actual trauma patients.

ACKNOWLEDGMENT

The authors would like to express their appreciation to General Motors of Canada Limited, the Premier's Research Excellence Award and Auto 21 for funding this work.

References

Abbreviated Injury Scale (AIS), American Association for Automotive Medicine, Morton Grove, Illinois. 1990.
Bowen I.G., Fletcher E.R., and Richmond D.R., "Estimate of Man's Tolerance to the Direct Effects of Air Blast", Technical progress report no. DASA-2113, DOD, Defense Atomic Support Agency, 1968.
Cronin D., Greer A., Williams K. and Salisbury C., "Numerical Modeling of Blast Trauma to the Human Torso", Proceedings of Personal Armor System Symposium, the Netherlands, 2004.
Cavanaugh J.M., Walilko T.J., Malhotra A., Zhu Y., and King A.I., "Biomechanical Response and Injury Tolerance of the Pelvis in Twelve Sled Side Impacts", 34th Stapp Car Crash Conference, 902305, 1990a.
Cavanaugh J.M., Walilko T.J., Malhotra A., Zhu Y., and King A.I., "Biomechanical Response and Injury Tolerance of the Thorax in Twelve Sled Side Impacts", 34th Stapp Car Crash Conference, 902307, 1990b.
Cavanaugh J.M., Zhu Y., Huang Y., and King A.I., "Injury and Response of the Thorax in Side Impact Cadaveric Tests", Proceedings of 37th Stapp Car Crash Conference, 933127, 1993.
Cavanaugh J.M., Walilko T., Walbridge A., Huang Y., and King A.I., "An Evaluation of TTI and ASA in SID Side Impact Sled Tests", Proceedings of the 38th Stapp Car Crash Conference, 942225, 1994.
Chung J., Cavanaugh J., King A., Koh S.W., Deng Y.C., "Thoracic Injury Mechanisms and Biomechanical Responses in Lateral Velocity Pulse Impacts", 43rd Stapp Car Crash Conference, SAE 99SC04, 1999.
Chang F., "The Development and Validation of a Finite Element Human Thorax Model for Automotive Impact Injury Studies", Proceedings of the ASME Int. Mech. Eng. Congress and Exposition, AMD-Vol. 251, 2001.
Deng Y.C., Kong W. and Ho H., "Development of a Finite Element Human Thorax Model for Impact Injury Studies", SAE International Congress and Exposition, SAE 1999-01-0715, 1999.
Eppinger R.H., Marcus J.H., Morgan R.M., "Development of Dummy and Injury Index for NHTSA's Thoracic Side Impact Protection Research Program", Government/Industry Meeting and Exposition, SAE 840885, 1984.
Furusu K., Watanabe I., Kato C., Miki K., Hasegawa J., "Fundamental Study of Side Impact Analysis Using the Finite Element Model of the Human Thorax", Japanese SAE Review, Vol. 22-2, 2001, pp. 195- 199.
Forbes P., Cronin D.S., Deng Y.C., "Multi-Scale Human Body Model to Predict Side Impact Thoracic Trauma", International Journal of Crashworthiness, V11:3, 2006.
Fung Y.C., Tong P., Patitucci P., "Stress and Strain in the Lung", ASCE Journal of the Engineering Mechanics Division, Vol. 104-No. 1, 1978, pp. 201-223.
Fung Y.C., Yen M.R., Zeng Y.J., "Characterization and modeling of thoraco-abdominal response to blast waves", University of California, San Diego, Contract No. DAMD17-82-C-2062, Vol-3, 1985.
Fung Y.C., Yen R.T., Tao Z.L., Liu S.Q., "A Hypothesis on the Mechanism of Trauma of Lung Tissue Subjected to Impact Load", Journal of Biomechanical Engineering, Vol. 110, 1988, pp 50-56.
Gayzik F.S., Hoth J.J., Daly M., Meredith J.W., Stitzel J.D., "A Finite Element-Based Injury Metric for Pulmonary Contusion: Investigation of Candidate Metrics through correlation with computed tomography.", proceedings of 51st Stapp Car Crash Conference, 2007, p189-209.
Greer A., Cronin D., Salisbury C., and Williams K., "Finite Element Modeling for the Predication of Blast Trauma", proceedings of IUTAM Symposium on impact biomechanics, Dublin, 2005.
Grimal Q., Watzky A., Naili S., "A one-dimensional model for the propagation of transient pressure waves through the lung", Journal of Biomechanics, Vol. 35-8, 2002, p1081-1089.
Happee R., Hoofman M., van den Kroonenberg A.J., Morsink P., Wismans J., "A Mathematical Human Body Model for Frontal and Rearward Seated Automotive Impact Loading", proceedings of 42nd Stapp Car Crash Conference, 983150, 1998.
Josephson L.H., Tomlinson P., "Predicted Thoraco-Abdominal Response to Complex Blast Waves", The Journal of Trauma, Vol. 28, 1988, S116-S124.
Kuppa S.M., Eppinger R.H., "Development of an Improved Thoracic Injury Criterion". Proceedings of 42nd Stapp Car Crash Conference, 1998, p.139-154.
Kroell C.K., Schneider D.C., Nahum A.M., "Impact tolerance and response of the human thorax II", proceedings of 18th Stapp Car Crash Conference, 1974.
Lau I.V., Viano D.C., "Thoracic Impact: A Viscous Tolerance Criterion", Proceedings of the 10th Experimental Safety Vehicle Conference, NHTSA, 1985, p104-113.

Lau I.V., Viano D.C., "The Viscous Criterion - Bases and Applications of an Injury Severity Index for Soft Tissues", Proceedings of the 30th Stapp Car Crash Conference, SAE, 861882, 1986.
Lee J.B., Yang K.H., "Development of a Finite Element Model of the Human Abdomen". Proceedings of Stapp Car Crash Conference, SAE 2001-22-0004, 2001.
Miller P.R., Croce M.A., Bee T.K., Qaisi W.G., Smith C.P., Collins G.L., and Fabian T.C., "ARDS After Pulmonary Contusion: Accurate Measurement of Contusion Volume Identifies High-Risk Patients", Journal of Trauma, vol. 51, 2001, p223-228, discussion 229-230.
Miller P.R., Personal Communication, April 1, 2008.
National Center for Statistics & Analysis (NCSA), National Highway Traffic Safety Administration, "Traffic Safety Facts 2006 (Early Edition)", DOT HS 810 818, 2006.
National Highway Traffic Safety Administration, "Federal Motor Vehicle Safety Standards; Side Impact Protection; Side Impact Phase-In Reporting Requirements; Proposed Rule, Federal Register, Part IV, Department of Transportation 49 CFR Parts 571 and 598", Docket No. NHTSA-2004-17694, 2004.
National Library of Medicine, "The Visible Human Project", National Institutes of Health, 2004.
Pintar F.A., Yoganandan N., Hines M.H., Maltese M.R., "Chestband Analysis of Human Tolerance to Side Impact", proceedings of the 41st Stapp Car Crash Conference, 973320, 1997.
Ruan J.S., El-Jawahri R., Chai L., Barbat S., Prasad P., "Prediction and Analysis of Human Thoracic Impact Responses and Injuries in Cadaver Impacts Using a Full Human Body Finite Element Model", Stapp Car Crash Journal, 2003-22-0014, 2003.
Ruan J.S., El-Jawahri R., Barbat S., Prasad P., "Biomechanical Analysis of Human Abdominal Impact Responses and Injuries Through Finite Element Simulation of a Full Human Body Model." Proceedings of Stapp Car Crash Conference, 2005-22-0016, 2005.
Salisbury C., Cronin D., Bouamoul A., Ouellet S., Williams K., "Numerical Investigation of Primary Blast Injury Protection Concepts", proceedings of Personal Armor Systems Symposium, 2006.
Stuhmiller J., Chuong C., Phillips Y., Dodd K., "Computer Modeling of Thoracic Response to Blast", Journal of Trauma, col. 28, 1988, S132-S139.
Sturdivan L.M., Viano D.C., Champion H.R., "Analysis of Injury Criteria to Assess Chest and Abdominal Injury Risks in Blunt and Ballistic Impacts", Journal of Trauma, vol. 56, 2004, p651-663.
Stitzel J.D., Duman S.M., Cormier J.M., Herring I.P., "A Non-Linear Finite Element Model of the Eye with Experimental Validation for the Prediction of Globe Rupture", proceedings of Stapp Car Crash Conference, SAE 2002-22-0005, 2002.
Stitzel J.D., Gayzik F.S., Hoth J.J., Mercier J., Gage H.D., Morton K.A., Duma S.M., Payne R.M., "Development of a Finite Element-Based Injury Metric for Pulmonary Contusion Part I: Model Development and Validation", proceedings of the 49th Stapp Car Crash Conference, 2005-22-0013, 2005.
Sparks J.L., Bolte J.H., Dupaix R.B., Jones K.H., Steinberg S.M., Herriott R., Stammen J., Donnelly B., "Using Pressure to Predict Liver Injury Risk From Blunt Impact", Stapp Car Crash Conference, 2007-22-0017, 2007.
States J.D., "The Abbreviated and the Comprehensive Research Injury Scales", proceedings of the 13th Stapp Car Crash Conference, 690810, 1969.
Takhounts E.G., Eppinger R.H., Campbell J.Q., Tannous R.E., Power E.D., Shook L.S., "On the Development of the SIMon Finite Element Head Model", 47th Stapp Car Crash Conference, SAE 2003-22-0007, 2003.
Thollon L., Arnoux P.J., Kayvantash K., Cavallero C., Brunet C., "Human Injury Evaluation using HUMOS RADIOSS Finite Element Model", IRCOBI Conference, 2002.
Viano D.C., Lau I.V., "A Viscous Tolerance Criterion for Soft Tissue Injury Assessment", Journal of Biomechanics. Vol. 21. 1988, p387-399.
Viano D.C., Lau I.V., Asbury C., King A.I., Begeman P., "Biomechanics of the Human Chest, Abdomen, and Pelvis in Lateral Impact", proceedings of the 33rd AAAM Conference, 1989a.
Viano D.C., "Biomechanical Responses and Injuries in Blunt Lateral Impact", proceedings of the 33rd Stapp Car Crash Conference, SAE 892432, 1989b.
Yang K.H., Beillas P., Zhang L., Lee J.B., Shah C., Hardy W., Demetropoulos C., Tashman S., King A.I., "Advanced Human Modeling for Injury Biomechanics Research", Digital Human Modeling for Design and Engineering Conference and Exposition, SAE 2003-01-2223, 2003.
Vawter D.L., "A Finite Element Model for Macroscopic Deformation of the Lung," Journal of Biomechanical Engineering, vol. 102, 1980.
Yen R.T., Fung Y.C., Ho H.H., Butterman G., "Speed of stress wave propagation in lung", Journal of Applied Physiology. 61(2), 1986, 701-705.
Yen R.T., Fung Y.C., Liu S.Q., "Trauma of Lung Due to Impact Load", Journal of Biomechanics, Vol. 21-9, 1988, p745-753.
Yen M., "Mechanical Properties of Human Heart, Lung, and Aorta for Highway Safety Research," Technical Report Sub-project F8C, The University of Memphis, Memphis, 1999.